Hindawi
Journal of Advanced Transportation
Volume 2022, Article ID 6428887, 15 pages
https://doi.org/10.1155/2022/6428887

Research Article

Optimal Deployment of Dynamic Wireless Charging Lanes for Electric Vehicles considering the Battery Charging Rate

Jun Du,[1] Mingyang Pei,[2] Bin Jia,[3,4] and Pan Wu[2]

[1]*School of Traffic and Transportation, Beijing Jiaotong University, No. 3 Shangyuancun, Haidian District, Beijing 100044, China*
[2]*Department of Civil and Transportation Engineering, South China University of Technology, Guangzhou 510641, China*
[3]*Institute of Traffic System Science and Engineering, Beijing Jiaotong University, No. 3 Shangyuancun, Haidian District, Beijing 100044, China*
[4]*School of Economics and Management, Xi'an Technological University, 58 Yanta Road, Xi'an 710000, China*

Correspondence should be addressed to Mingyang Pei; ratherthan@foxmail.com and Bin Jia; bjia@bjtu.edu.cn

Received 19 December 2021; Revised 23 July 2022; Accepted 18 August 2022; Published 21 September 2022

Academic Editor: Lina Kattan

Dynamic wireless charging (DWC) technology enables the charging of electric vehicles (EVs) en route without the need for stopping on long-distance trips. Based on DWC technology, a dynamic wireless charging system (DWCS) concept is proposed to determine the number of DWC lanes and their locations and lengths considering varying battery charging rates. A two-stage approach is proposed to design the optimal DWCS. First, we propose a mixed-integer model with nonlinear constraints to determine the locations and lengths of the charging lanes. This model is further reformulated as a mixed-integer linear problem to make it suitable to solve with off-the-shelf commercial solvers (e.g., Gurobi). Next, we propose a method to obtain an approximately optimal solution for the number of lanes. Then, a numerical example from a freeway in Guangdong Province, China, is investigated to demonstrate the applicability of the proposed model and its effectiveness in reducing the construction costs.

1. Introduction

Electric vehicle (EV) deployment has grown rapidly over the past ten years [1], with the global stock of electric passenger cars passing 5 million in 2018, corresponding to an increase of 63% from the previous year [2]. However, a typical EV has a limited driving range and a long charging time, hindering the large-scale adoption of EVs. Deployment of EV charging infrastructure on long-distance roads will significantly reduce current vehicle energy consumption [3–6], make transportation more environmentally friendly [4, 5], and relieve long-distance power anxiety [7–10].

Emerging wireless charging (WC) technology holds the promise of overcoming these issues [11–13]. With this technology, the EV's battery is charged via wireless power transfer (WPT) technology [14, 15]. WPT is an emerging and promising technology that was introduced by Nikola Tesla in the 19th century and over time has evolved to become a competitive solution with wired charging systems [11]. This technology can replace plug-in interfaces through transmitters and receivers, allowing the flow of energy in the form of electromagnetic or static waves in a noncontact manner. The wireless charging system can operate without human intervention. It is also safe from the dangers caused by the use of cables. The main drawback of the wireless charging system is its charging time, which can be solved by different variations in the system. For electric vehicles, WPT can be performed in three modes: (1) stationary wireless charging (SWC), (2) dynamic wireless charging (DWC), and (3) quasidynamic/stationary wireless charging (QDWC). SWC is the method of charging an EV when the EV is parked and not operational for an extended period at a stationary point. SWC technology is maturing [16]. SWC makes the charging process safer and more convenient. However, SWC is not significantly different from the traditional plug-in conduction charging in terms of charging time, frequency, vehicle operation, and charging station assignment. Due to the limitation of battery capacity, electric vehicles need more charging cycles to travel longer distances

[17]. This problem can be solved by DWC [18]. In DWC, the transmitter mat is placed on a small section of pavement and the receiver mat is placed on the EV chassis to provide charging for the moving EVs. This technology requires a significant capital investment. Moreover, the implementation of the DWC system must consider the speed of the vehicle. QDWC has some of the advantages of DWC. However, it requires less investment compared to DWC. The QDWC mode provides charging to the EV when it is stationary or when it is moving slowly for short time. This method is suitable for charging public transportation EVs when they stop at bus stops or cab stands, or traffic signals. In this method, the battery is not fully charged [19]. The flexible nature of the WPT technology makes it suitable for commercial purposes. Several methods can be used for WPT. The various methods depend on the technology used and the frequency level of the transmission. Accordingly, WPT can be divided into two types: (1) coupled (near field) and (2) radiated (far field). Coupled systems are further divided into systems using either magnetic or electric field radiation. The coupled types are further split into two categories: microwave and laser.

As shown in Figure 1, a WC system makes use of the charging infrastructure (e.g., electricity grid and magnetic coil) embedded under the surface of the road that transfers electric power to a vehicle's inductive pick-up component while it is in transit. Specifically, a new technology for dynamic wireless charging to help electric vehicles recharge on the go has been undergoing trials in Dubai. One of the most active players in stationary and dynamic charging is the wireless technology juggernaut Qualcomm that recently developed and tested one of the world's first DEVC test tracks, as shown in Figure 1(a). This system is capable of charging an EV dynamically at up to 20 kW at highway speeds (100 km/h). The demonstrations took place at the 100-meter test track at Satory Versailles, recently built by the French research institute VEDECOM as part of the FABRIC project. The Qualcomm Halo DEVC system was integrated into the test track, and the receiving components were installed in two Renault Kangoo EVs. A schematic of the test setup is presented in Figure 1(b) and shows that the Dubai test road can charge moving vehicles based on the power-charging grid underneath a 60 m road strip at the Dubai Silicon Oasis. Wireless power transfer (WPT) theory is shown in Figure 1(c), that is, the underground power-charging grid transmits electrical power to a magnetic coil in contact with the vehicle, and then, the electrical power is transmitted through the magnetic coil to the battery of the moving vehicle [20–22]. WPT is achieved by resonant compensation, allowing it to reach high transmission efficiency comparable to that of wired charging systems [23, 24]. This is a key point that enables the adoption of WPT [25, 26].

WC is not a novel concept; it was first presented by Bolger in 1978 and involved the collection of electric energy transferred from a source embedded in a roadway [29]. WC technology mainly comprises two categories: dynamic (i.e., charging while driving) and static (i.e., charging while the vehicle is stationary/parked) [4, 14]. High-power (e.g., 60–120 kW) static WC has been demonstrated worldwide on electric transit buses since 2002 [30]. Emerging dynamic wireless charging (DWC) technology, in which a vehicle is inductively charged as it moves along the roadway, extends the vehicle range and reduces or eliminates the need for frequent stops to recharge. WC technology is being developed and tested worldwide. Figure 1(b) shows a DWC lane demonstration from Qualcomm Halo DEVC. This technology has been successfully demonstrated on a test basis at the Formula E championship using a BMW i8 vehicle [27]. A charging lane of 15 miles has already been established in Gumi, South Korea [31], Scania and Siemens are working together on overhead charging technology and conducting a 2 km test outside Berlin [32], Volvo is conducting field tests of two conductive charging technologies with a total number of 20 vehicles in Goteborg, Sweden [33], and an electric vehicle and bus test line have been constructed at the Dubai Silicon Oasis [28] (as shown in Figure 1(a)). These test results from the industry proved that highly efficient wireless charging system with effectiveness comparable to that of cable charging are now available [28]; thus, WC technology is being realized, to enable electrical charging of private vehicles similar to trolleys [34]. Moreover, they found that for an electric vehicle with a 24 kWh battery, dynamic charging at 25 kW, and 40% road coverage, a driving range of 310.6 miles can be achieved. They also simulated battery charging states for different driving cycles on different roads to estimate the range of increase due to various dynamic charging levels and efficiencies. For an electric vehicle with a 24 kWh battery and a 90% dynamic wireless charging system (DWCS) with 20% road coverage, the estimated expected range extension was between 12% (10 kW) and 217% (40 kW) based on the drive cycle [30].

Although the DWC is considered to be an excellent approach to reduce range anxiety and encourage EV use, the construction cost of DWCSs (e.g., installing power transmitters and constructing DWC lanes) is quite high. For example, California's cost estimates for a single dynamic charging lane range from 2.3 to 3.2 million dollars per mile, and for dynamic charging electric vehicles at 100 kW, the use of an approximately 240-mile-long charging lane is required [30]. To reduce the construction cost and maximize the utility and benefits of DWCSs, this paper proposes a structural design method for DWC lane construction. The optimization problem is generally defined in two components.

(i) First, as shown in Figure 2(a), the construction cost can be reduced by optimizing the locations of the charging segments and power transmitters

(ii) Second, according to each charging section's real volume, particularly in some overvolume scenarios, the construction cost can be further reduced by minimizing the number of lanes. This process includes allocating charging lanes and strategies for individual drivers for overloaded travel demands, as shown in Figure 2(b)

2. Literature Review

Since public power infrastructure plays a critical role in EV systems [4, 9, 35] and the envisioned maturity of DWC technologies [36], a handful of studies have investigated the deployment

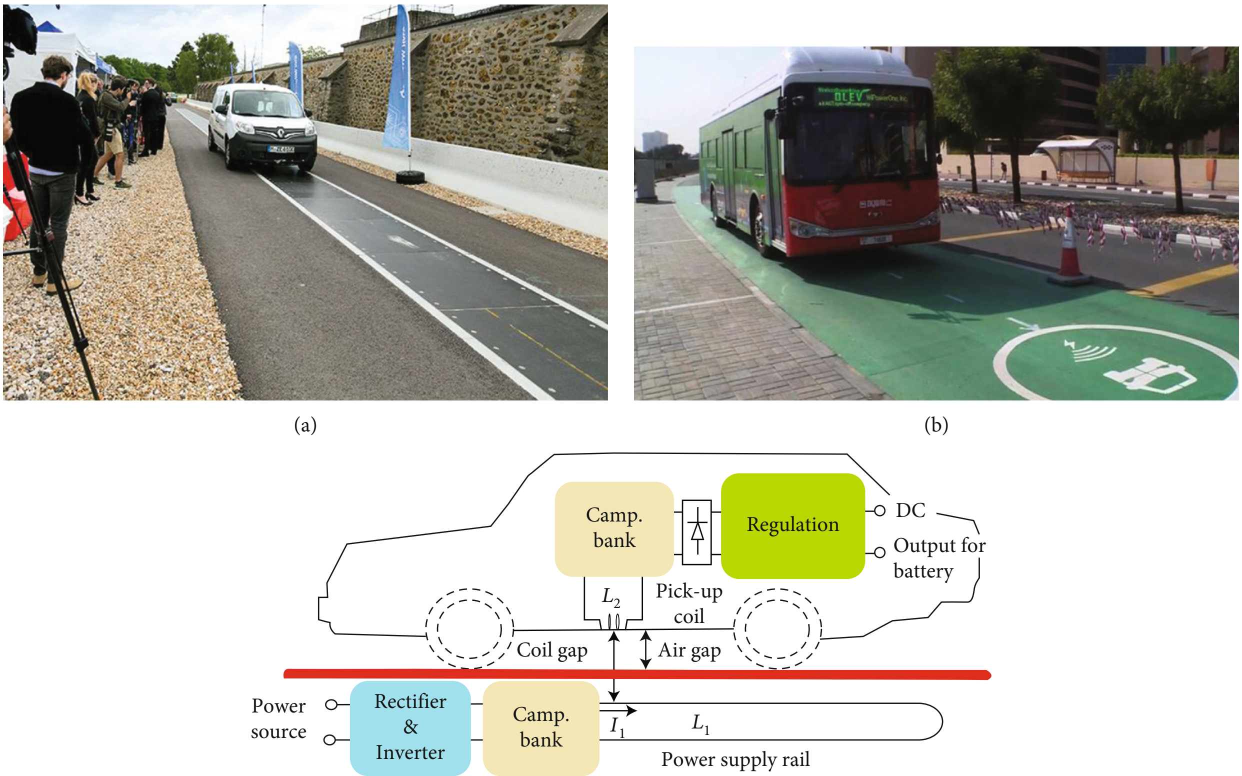

(a) (b) (c)

Figure 1: DWC vehicle on a test track and fundamental theory. (a) Source from Qualcomm Halo DEVC [27] and (b) Dubai Silicon Oasis charge vehicles [28]. (c) Source from 2GreenEnergy [20].

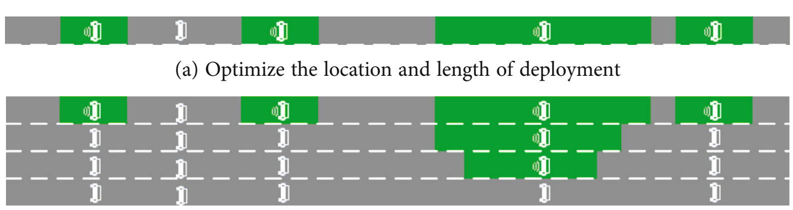

(a) Optimize the location and length of deployment

(b) Reduce the number of charging lanes (overload travel demands)

Figure 2: Stretch of optimized DWC lanes in this paper (the marked green lanes are the designed DWC lane that allows EVs to run and charge simultaneously).

of DWC infrastructure. The investigated WC technology holds the promise of realizing long-distance freeway travel without the need for recharging stops [34, 36–41]. Several recent studies are aimed at designing a DWCS to serve an EV charging corridor. However, most existing DWC systems rely on bus transit, for example, in the studies of a single route [36, 42–46] and multiple routes [3, 5, 40]. Meanwhile, only a few studies consider other types of vehicles [4], [30, 39, 47] with multiple routes and heterogeneous origins-destinations (ODs). A comprehensive review article by Jang [14] concluded that three types of decision modeling approaches are adopted in DWCS operation and planning. Table 1 compares the three types of modeling approaches. The first approach is a continuous variable approach [37, 40, 42, 48], in which the allocation of the charging lane is modeled as a set of continuous variables (x_i^o, x_i^f). The second approach uses the segmented discrete binary variable $x_i = \{0, 1\}$, in which the DWC lane has been extended by discretizing the route into multiple small segments [3, 5, 42, 44–46]. The third approach uses a link variable x_{ij} representing a specific link [4, 30]. The solution algorithms to relevant DWCS design problems can generally be classified into two types, i.e., heuristic algorithms such as particle swarm optimization [3, 40, 42, 43] and genetic algorithm [44, 45, 49] and mathematical programming methods, mainly including existing commercial solvers (e.g., CPLEX, GAMS, and Gurobi) [30, 39, 43, 46, 50] and customized algorithms [4]. These modeling approaches have achieved better results in optimizing the deployment of DWC systems, but some issues still need to be addressed. For example, the location and length of the charging lanes were not considered in the optimization of DWC systems. Although the optimization algorithms used to date can achieve the expected results, they are still complex and computationally

Table 1: Summary of recent studies in DWC facility deployment modeling approaches.

Scale	Variable	Notation	Sketch	References
Corridor	Continuous	$\left(x_i^o, x_i^f\right)$	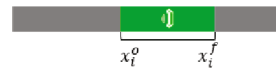	[37, 40, 42, 48]
	Segmented discrete	x_i	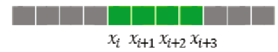	[3, 5, 44]–[46]
Network	Link	x_{ij}	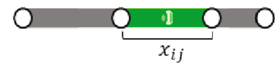	[4, 30]

difficult. Moreover, the electric transit bus system also utilizes wireless power transfer technology. Inspired by these studies, we propose a novel optimization approach for multiple types of vehicles with multiple lanes. The optimization method is implemented in two stages: the charging lane location and length are optimized and the minimum number of lanes is reduced by organizing the individual charging strategies. This two-stage approach can significantly decrease the algorithm complexity and quickly obtain a real-case acceptable solution.

A DWCS is an attractive system for future transportation because it does not rely on large and heavy batteries but rather directly and efficiently supplies power to vehicles as the vehicles move along a road [51]. Researchers have proposed optimization strategies to minimize battery size [40] and energy consumption [52]. Despite these pioneering explorations, there is a lack of a general method for DWCS design over DWC lanes considering the battery charging rate. Most of the previous studies are roughly linear between the maximum and minimum charging points [36, 42, 43, 53]. Considering the complicated nonlinearity spectrum of battery charging, some simulation results have been obtained for the health-aware fast charging strategy for lithium-ion batteries (LIBs) [54, 55]. In the nonlinear charging function, the charging speed decreases approximately linearly over time [36, 56–58]. Because the charge curve of an LIB is complicated and closely related to the charging efficiency, the charging speed and curve are introduced as a framework that can be further replaced and discussed.

3. Contributions

This paper focuses on the design of an operational DWCS to reach a minimum construction cost of deployment of charging segments and power transmitters while considering construction of multiple lanes for overloaded travel demands. Different from previous studies, this paper makes three main contributions:

(i) First, this paper develops a DWCS model considering the varying battery charging rate in the infrastructure planning process. The EVs can be optimized to charge at the best SOC point by considering the charging speed rate, thus improving energy efficiency.

(ii) Second, this paper proposes a method to lower the construction cost of multiple lanes for overloaded travel demands. Moreover, multiple OD pairs with various battery power levels are given different charging strategies in this process from those used in previous studies. These charging strategies can help reduce the number of charging lanes.

(iii) Third, the optimization of the charging lane location and length with multiple lanes is difficult in large real-case applications. This paper proposes a two-stage division method that can significantly decrease algorithm complexity and quickly obtain an acceptable real-case solution.

Overall, this work gives the DWCS significant insights on the future integration of EVs into long-distance freeway services and a numerical technique for building the ideal operating plan for this integrated system. The remainder of this paper is organized as follows. The operating features, nomenclature, and idea of the proposed DWCS are introduced in Section 2. Section 3 builds a mixed-integer nonlinear programming model to optimize the locations and length of charging lanes. Section 4 proposes a methodology to reach an approximately optimal solution with respect to the number of lanes. Finally, Section 5 states the conclusions and recommends future research directions.

4. System Description

This section introduces the operational process of the DWCS and the underlying assumptions. For the convenience of the readers, we present the notation for the critical parameters and variables in Table 2 below. Consider a DWC corridor discretized into a set of segments $\mathscr{M} \coloneqq \{1, \cdots, M\}$. Let the binary variable x_m denote whether segment m is selected as a DWC charging segment. As shown in Figure 3, only one transmitter is needed for each set of consecutive selected segments. To evaluate the power transmitter, we introduce another binary variable, y_m, that denotes whether segment m is the start segment of the WC lane [5, 43]. We set $y_m = 1$ if and only if $x_{m-1} = 0, x_m = 1$, denoting that segment m is the start segment of the wireless charging lane. To represent these conditional constraints, as shown in Equations (1)–(3), we use the definitions of x_m and y_m above.

$$y_1 = x_{1,} \tag{1}$$

$$x_m - x_{m-1} \le y_m \forall m \in \mathscr{M} \setminus \{1\}, \tag{2}$$

Table 2: Notation.

Sets	Descriptions of variables
$\mathscr{M}$	Set of segments, $\mathscr{M} \coloneqq \{1, \cdots, M\}$
$\mathscr{U}$	Set of vehicle trip character index, $\mathscr{U} \coloneqq \{1, \cdots, U\}$
Parameters	
u	Index of vehicle trip character, $u \in \mathscr{U}$
m_u^+	Departure location for vehicle trip character index u
m_u^-	Destination location for vehicle trip character index u
p_u^0	Initial battery capacity for vehicle trip character index u
C_1	Fixed construction cost per segment (¥)
C_2	Fixed cost of a set of power transmitters (¥)
s	Energy cost per segment
f	The formula for battery capacity with charging speed
l	Distance per segment
v	Average vehicle travel speed
p^H	The upper limit of the battery capacity level
p^L	The lower limit of the battery capacity level
Decision variables	
x_m	Binary variables, $x_m = 1$ when a segment m is selected as a wireless charging lane, $x_m = 0$, otherwise
y_m	Binary variables, $y_m = 1$ when the segment m is the start segment of the wireless charging lane, $y_m = 0$, otherwise
$p_{u,m}$	Continuous variables, current battery power for vehicle trip character index u at the beginning of segment m when $m \le M$
$\tau_{u,m}$	Continuous variables, average charge amount for vehicle trip character index u at segment m
$r_{u,m}$	Continuous variables, amount of excess power in the segment m for vehicle trip character index u
$w_{u,m}$	Continuous variables, $w_{u,m} = \tau_{u,m} * h_{u,m}$ in the linearization process

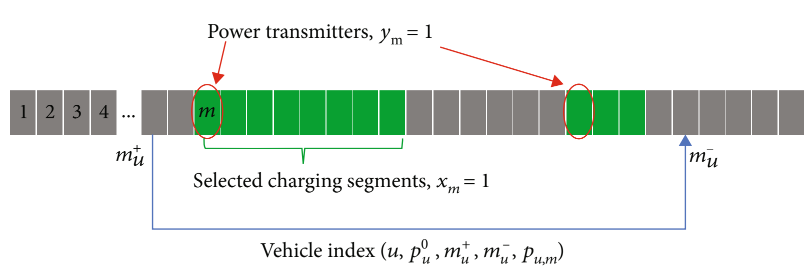

Figure 3: DWC lane infrastructure diagram.

$$y_m \le \frac{1}{2(x_m - x_{m-1})} + 1/2 \forall m \in \mathscr{M} \setminus \{1\}. \tag{3}$$

Consider a set of vehicle trip character indexes, $\mathscr{U} \coloneqq \{1, \cdots, U\}$ such that the trip for vehicle u starts at origin m_u^+ with the original power charging level of electric battery p_u^0 and ends at destination m_u^-. Let continuous variable $p_{u,m}$ denote the current power charging level for vehicle u at the beginning of segment m when $m \le M$. Since the charging rate is not a constant parameter [45], we introduce another continuous variable $\tau_{u,m}$ to denote the average charging amount that a vehicle u incurs through a segment m. Figure 4 shows the charging (red curve) and discharging (green curve) processes for vehicle u, where the battery charging rate of a vehicle depends on its current battery power level $p_{u,m}$.

In some previous studies [47, 57], the charging rate is assumed to be a concave function that satisfies $f(p_{u,m}) > 0, f'(p_{u,m}) < 0$. Moreover, $f(p_{u,m})$ can be replaced with any latest charging speed function. To obtain the charging amount of vehicle u at segment m, we use the average charging speed $(f(p_{u,m}) + f(p_{u,m+1}))/2$ multiplied by the charging time l/v. Let l denote the distance for a discrete charging segment and let v denote the average vehicle travel speed for the EV. Formulas $f(p_{u,m})$ and $f(p_{u,m+1})$ denote the charging rate of the current

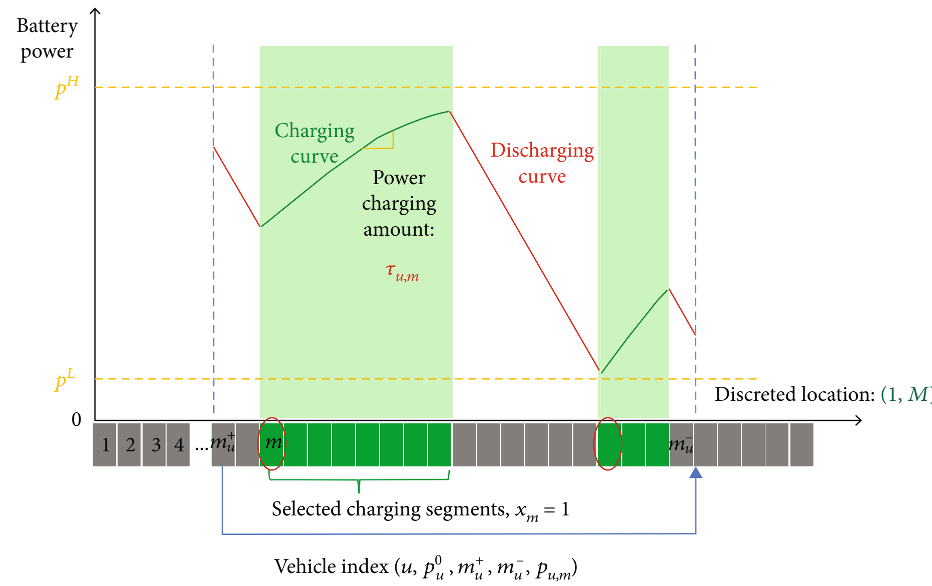

Figure 4: Charging and discharging curves.

power level $p_{u,m}$ at the beginning and end of segment m, respectively, as shown in Equation (4).

$$\tau_{u,m} = \frac{f(p_{u,m}) + f(p_{u,m+1})}{2} * \frac{l}{v} \forall m \in \mathcal{M}, u \in \mathcal{U}. \quad (4)$$

The battery power level should be in the range set by the lower limit of the battery capacity level p^L and the upper limit of the battery capacity level p^H. Equation (5) shows that the current battery power level must be in this power level range.

$$p^L \leq p_{u,m} \leq p^H m_u^+ \leq m < m_u^-, \forall u \in \mathcal{U}. \quad (5)$$

The lower power level limit is set to fit the safety constraints, while the upper power level limit is set to prolong the life of the vehicle's battery [40, 42, 43]. A vehicle in the charging lanes cannot enter and leave at every point because of the organizational difficulties and billing problems in a real-world application. This paper only allows vehicles to enter at the beginning of a charging lane and leave at the end of a charging lane or at toll stations in the internal WC lane. Due to the limited access to the charging sections, we further define a continuous variable $r_{u,m}$ as the amount of excess power on segment m for vehicle u. As presented in Figure 5, the green curve shows the current battery power in each charging segment, and the vehicle stops charging and maintains the upper power limit in the charging segments. In our model, this excess charging power is also taken into consideration.

We introduce the following assumptions in the investigated problem to facilitate the model formulation.

Assumption 1. First, we assume that the power consumption of EVs is proportional to the driving distance [59]. It is difficult to relax this assumption because capturing speed selection in charging lanes appears to be mathematically intractable [4].

Assumption 2. Second, we assume that all of the vehicle drivers in this system are rational and always follow the guidance. This assumption can be easily relaxed when the EV in this system is replaced by autonomous electric vehicles (AEVs) in the future [60].

Assumption 3. All vehicles in our system have no less than a specific battery capacity (i.e., the minimum battery capacity size is from the market and EV government design instruction). This assumption is designed for safety constraints.

5. Methodology

5.1. Stage 1: Deploy the Location and Length. In this section, we develop a DWCS lane location and length model to optimize the construction cost considering a varying battery charging rate. This proposed DWCS model is initially formulated as a mixed-integer nonlinear programming model. To facilitate its solution efficiency, the model is further reformulated into a mixed-integer linear problem that can be solved by off-the-shelf commercial solvers to obtain the exact solution.

5.1.1. Objective Function. The objective function formulated in Equation (6) is aimed at minimizing the DWCS infrastructure investment cost. It includes two cost components for installing the power transmitters ($C_1 \sum_{m \in \mathcal{M}} x_m$) and constructing the DWC lane ($C_2 \sum_{m \in \mathcal{M}} y_m$). This cost is translated into the construction cost of several segments of charging lanes and the power transmitter construction cost in the segmented approach. The charging segment construction cost in the construction process, denoted by C_1, includes the materials cost and labor cost and is the cost when segment m is selected as a dynamic charging segment. The power transmitter construction cost, denoted by C_2, is the cost associated with the number of connected charging lane segments. We assume that a single power transmitter

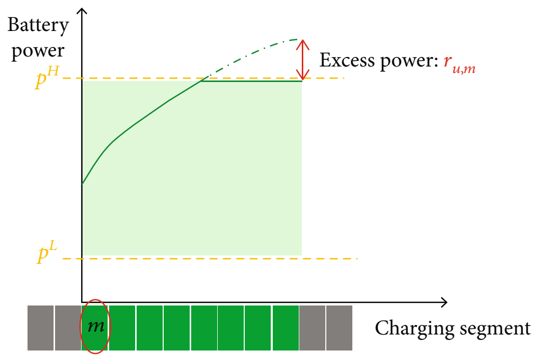

Figure 5: Diagram of excess power.

construction cost is fixed and that the costs of the selected charging lanes are linear. When the charging segment is connected, it can share a transmitter.

$$\min F \coloneqq C_1 \sum_{m\in\mathscr{M}} x_m + C_2 \sum_{m\in\mathscr{M}} y_m \quad (6)$$
$$\text{s.t.constraints } (1-5) \text{and } (7-12).$$

5.1.2. Power Level Constraints. For each vehicle index u, the current power level at departure point m_u^+ is p_u^0. $r_{u,m}$ is a continuous variable and denotes excess power in segment m for vehicle u. Let s denote the energy cost of a segment. Let $m+1$ denote the ending point of segment m, and then, the current power level $p_{u,m}$ can be calculated by recursive formulation (8).

$$p_{u,m_u^+} = p_u^0 \forall u \in \mathscr{U}, \quad (7)$$

$$p_{u,m+1} = p_{u,m} - s + \tau_{u,m}x_m - r_{u,m}\ m_u^+ \le m < m_u^-, \forall u \in \mathscr{U}. \quad (8)$$

We note that constraint (8), $\tau_{u,m}x_m$ is a bilinear term. It is well-known that mathematical programming with a bilinear term is difficult to solve directly. To facilitate the solution approach, this section reformulates the component $w_{u,m} = \tau_{u,m}x_m$ to a linear term via the following constraints (9)–(12). A large given number G is introduced in formulation (12). Constraints (9) and (10) ensure that the value of $w_{u,m}$ is identical to $\tau_{u,m}x_m$. This is because when $x_m = 0$, constraints (9) and (10) always hold for all feasible values of $w_{u,m}$ allowed by the demand and thus are not activated; only when $x_m = 1$ does constraint (9) yield $\tau_{u,m} \le w_{u,m}$ and constraint (10) yield $w_{u,m} \le \tau_{z,m}$, and thus, $w_{u,m} = \tau_{u,m}x_m$. Constraints (11) and (12) specify each $w_{u,m}$ as a positive continuous variable.

$$\tau_{u,m} + G(x_m - 1) \le w_{u,m} \forall m \in \mathscr{M}, u \in \mathscr{U}, \quad (9)$$

$$w_{u,m} \le \tau_{z,m} + G(1 - x_m) \forall m \in \mathscr{M}, u \in \mathscr{U}, \quad (10)$$

$$0 \le w_{u,m} \forall m \in \mathscr{M}, u \in \mathscr{U}, \quad (11)$$

$$w_{u,m} \le G x_m \forall m \in \mathscr{M}, u \in \mathscr{U}. \quad (12)$$

For each $d \in D$, dose
  Let $p_d^{\text{low}}(d) = p^L$, $i = d$
  While $i > 1$
   $i = i - 1$
    If $x_i = 0$
     $p_d^{\text{low}}(i) = p_d^{\text{low}}(i+1) + s$;
    Else if $x_i = 1$
    Solve $p_d^{\text{lim}}(i)$ through equations below
   $p_d^{\text{low}}(i+1) = p_d^{\text{low}}(i) + \tau_m - s$
   $\tau_m = f_{u,m} + f_{u,m+1}/2 * l/v$
   End if
  End while
End for

Algorithm 1: General p_d^{low}.

With the above linearization steps, the investigated DWCS problem is reformulated as an MILP model with objective (6), subject to vehicle capacity constraints (2)–(5) and (7)–(12).

5.2. Stage 2: Reduce the Number of Charging Lanes. Motivated by the potential overloaded travel demands in some charging segments, we propose a methodology to optimize the number of DWC lanes and simultaneously allocate the individual charging strategies. In this section, multiple OD pairs with various battery power levels are given different charging strategies. This approach can guarantee that the battery power level is not lower than the lowest power safety band. The methodology can be summarized in Algorithms 1–3 that are used to reach an approximate optimal solution in the operation process.

There is a minimum initial battery power level for each OD pair, and vehicles with this battery power level (or higher) can proceed through their trip in our DWCS. Let $o \in \mathscr{O}$ denote the departure station set and $d \in \mathscr{D}$ denote the destination set. Let $p_d^{\text{low}}(d)$ denote the minimum power level of the destination d that must be larger than the lower battery power limit p^L. Algorithm 1 shows the methodology to back-step to the minimum $p_d^{\text{low}}(i)$, $i \in \mathscr{M}$ of each intermediate point to the departure points. Similarly, Figure 6 shows the minimum battery level required for each vehicle in a specific location determined by the back-stepping method.

The charging rate in this paper is a concave function that satisfies $f(p_{u,m}) > 0, f'(p_{u,m}) < 0$, which means that the delay-charge strategy will obtain a higher reward (average charging efficiency is higher). As we have already calculated the minimum $p_d^{\text{low}}(i)$, $i \in \mathscr{M}$, in stage 1, a vehicle in this DWCS can stop charging if its battery satisfies the constraint $p_{u,m+1} - s > p_d^{\text{low}}(m+1)$. This delay-charge strategy can significantly reduce the low-efficiency charging preference and decrease the unnecessary charging demand volume. More details are shown in Algorithm 2 below. Let u_1 denote the vehicle index with the OD information. Consider a new set $\mathscr{N} \coloneqq \{1 \cdots .n \cdots N\}$ that denotes the potential connecting charging segments to be selected (following the same rules from Section 2). Let in_n and out_n denote the beginning and ending points of connecting charging segment n, respectively. Then, let the binary variable

```
For each d ∈ D, and u_1,
    If m^-_{u_1} = d
     i = m^+_{u_1}
       While (i < m^-_{u_1})
       p(u_1, i + 1) = p(u_1, i) − s
            If            p(u_1, i + 1) < p_d^low(i) and in_n ≤ i ≤ out_n
            Update p(u_1, in_n + 1 : out_n)
            h(u_1, n) = 1
            i = out_n
            End if
       i = i + 1
            End while
    End if
End for
```

Algorithm 2: Calculate $p_{u_1,m}$ and $h(u_1, n)$.

```
For n = 1 : N
   Q(n) = 0
      For u_1
            Q(n) = Q(n) + h(u_1, n) *
      data(u1)
      End for
End for
num(n) = ceil (Q(n)/vol)
```

Algorithm 3: Calculate num(n).

$h(u_1, n)$ denote whether vehicle index u_1 chooses to charge at each segment n.

Let Q_{vol} denote the design traffic volume for a single lane; then, we can obtain the cumulative charging demand volume in each connecting segment. More details are shown in Algorithm 3 below.

Multiple OD pairs with various battery power levels are given different charging strategies using the above-described methodology. We assume that all vehicles follow the charging instructions, which is not considered to be a strict assumption in the future CAV environments. These charging strategies can help reduce the number of charging lanes and reduce the low-efficiency energy usage. Although this methodology of calculating the number of lanes is not an ideal approach to reaching an exact optimal solution, this simple methodology with high calculation speed does improve the charging strategies (i.e., choosing optimal charging lanes and reducing the necessary charging period) and reduces the number of the DWC lanes. The use of an integrated model that includes the location, length, and number of lanes risks solution failure even with two-node OD demands. In future studies, we will focus on this point, establish a more general model, and find an optimal result with precise algorithms.

6. Numerical Example

To illustrate the application of the proposed model, this section investigates a numerical example from the Guangdong Province freeway. The constructed route OD pairs ranged over 305 km. In this example, we select 22 toll stations as potential ODs. The initial battery levels of vehicles are a doubly truncated normal distribution (classified into seven categories). Figures 7 and 8 show the station locations and hourly OD demand, respectively.

All experiments were performed on a PC with an Intel® Core™ i7-8550U @1.99 GHz CPU and 24 GB RAM. The code was implemented in MATLAB 2019a and uses the commercial MILP solver Gurobi [61–63]. The charging rate we used is fit to a linear function [47, 57], and in this paper, we select the parameters considering both the vehicle battery characteristics and electric grid characteristics, such that $f(p_{u,m}) = 0.6 - 0.3 * p_{u,m}$. Other default parameter values are given in Table 3.

6.1. Result of Stage 1: Location and Length. As shown in Figure 9, the optimal DWC lanes have six connected segments, i.e., locations 19 to 36, 50 to 79, 101 to 129, 150 to 178, 199 to 232, and 256 to 284. Figure 9 shows the charging and discharging curves of the heterogeneous vehicles.

The operation cost is very important in a charging system. However, this study does not involve operating costs. Specifically, we only consider the appropriate choice of a setup by the government of a charging strip. For example, in the case of a highway shown in Figure 7, it would be more expensive to lay the entire strip. However, if only some of the strip would be set up for charging, it is difficult to determine which part should be used for charging in order to minimize the cost and whether a single-lane charging strip or a two-lane charging strip is needed. This paper is dedicated to solving these challenges.

We are focusing on wireless charging roadway rollout and charging strategies. Here, the objective function contains two contributions to the cost. The first is the price per kilometer laid, and the second is the price paid per section laid and does not include operating costs. The cost is considered in this manner in order to fully reflect the fact that the cost of a wireless charging section is related to the distance, and the cost is related to the number of sections laid. This method of calculating has already been verified in reference [40]. The first contribution is the price per kilometer laid, and the second contribution is the price per

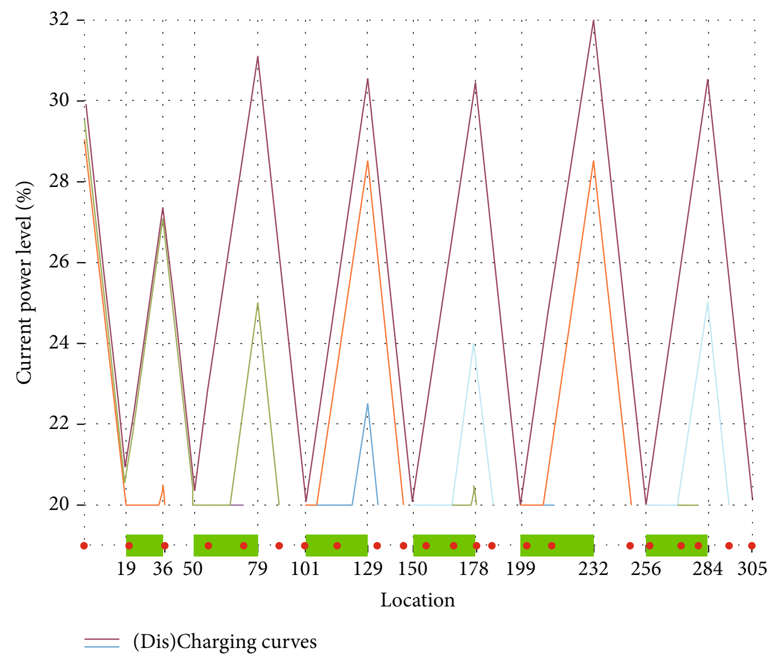

Figure 6: Minimum battery level for u.

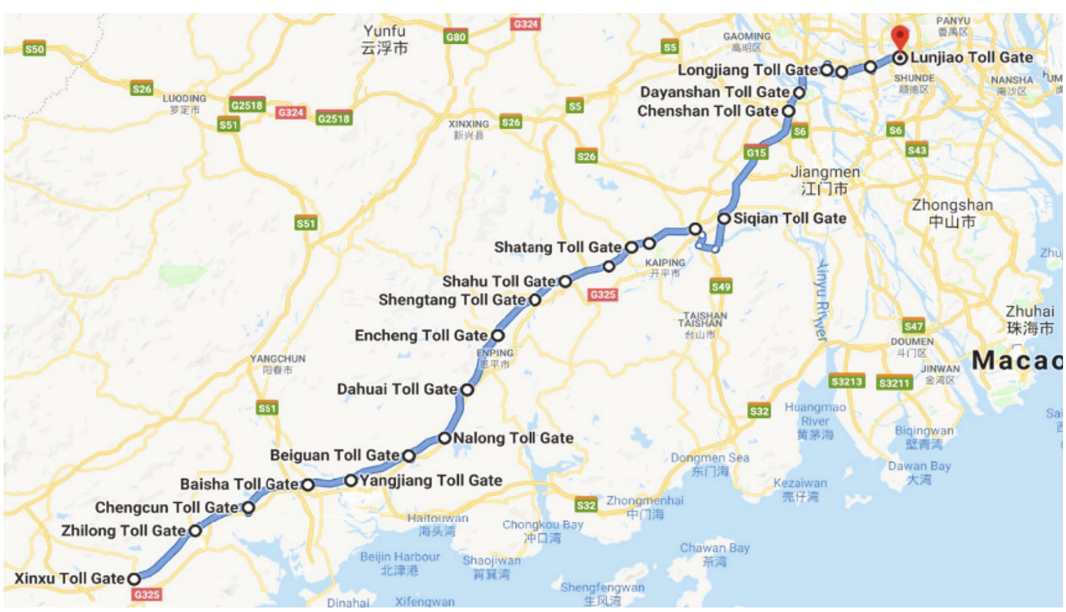

Figure 7: Toll station locations.

section laid, not including operating costs. This setting cleverly and reasonably avoids the duplicate construction of charging support facilities and grid distribution lines, etc., caused by the fact that the number of charging strips will be exceptionally large and each section will be very short.

For the case shown in Figures 7 and 8, our final solution results in a total of 6 charging belts, each of which is shown as a thick green line in Figure 9. After our stage 2 planning, all of them can be built as single-lane charging belts to satisfy the traffic. The cost of 163 km is 163 ∗ 1 million + 6 ∗ 2 million = 175 million.

6.2. Result of Stage 2: Number of Lanes. All vehicles choose whether to charge when they have access to charging. The results show that some vehicles only charge to the minimum power level to reach the next charging section, indicating the efficiency of the design. It is observed from Figure 7 that the number of DWC lanes on a charging section generally increases with the charging demand (e.g., sections 50-79, 199-202, and 272-284 with higher demand are assigned with more DWC lanes).

As shown in Figures 10(a) and 10(b), after using the proposed method, the charging demand volume is distributed

	XX	ZG	CC	BS	YJ	BG	NL	DH	EC	ST	SH	TK	ST	KP	SK	SQ	CS	DYS	LJ	XT	LL	LJ
XX	0	599	59	72	144	28	37	15	7	24	3	3	9	4	11	5	5	7	2	4	14	4
ZG	535	0	80	91	723	38	13	21	3	13	7	8	11	3	8	4	2	1	3	4	18	3
CC	65	62	0	49	206	63	29	3	0	2	0	3	3	4	10	2	0	0	0	1	2	0
BS	59	74	31	0	1153	791	275	29	10	12	5	5	9	7	25	10	3	4	2	3	7	2
YJ	151	726	229	1113	0	699	237	72	29	40	10	20	17	34	22	15	9	5	12	3	35	5
BG	65	35	102	741	630	0	23	21	11	11	3	5	10	12	13	6	0	2	2	1	5	2
NL	62	22	41	236	199	24	0	35	17	8	1	6	5	6	18	2	3	2	0	4	4	1
DH	11	12	5	23	71	23	32	0	73	33	12	6	9	11	7	5	2	1	2	0	3	1
EC	5	5	2	6	37	11	15	69	0	108	94	36	50	115	45	41	21	19	13	2	28	7
ST	20	10	2	13	25	6	5	26	86	0	24	26	40	62	112	42	20	12	8	11	27	8
SH	4	3	2	8	7	6	7	10	95	41	0	51	86	50	137	33	6	7	2	4	16	6
TK	2	3	2	6	10	2	1	9	18	23	32	0	109	38	79	24	13	5	6	3	19	6
ST	9	10	2	5	10	10	3	15	31	42	95	84	0	26	171	53	12	7	4	5	9	5
KP	5	4	2	10	35	8	12	11	107	68	48	29	31	0	468	82	41	13	18	9	68	11
SK	18	9	9	18	32	16	14	28	60	169	281	136	187	508	0	51	74	32	34	18	78	14
SQ	5	2	3	10	15	12	4	5	47	44	36	19	48	91	33	0	36	17	21	15	29	12
CS	2	1	1	1	11	2	0	4	15	14	5	8	7	31	60	32	0	48	125	38	135	43
DYS	2	1	1	4	6	0	2	1	17	12	6	5	3	26	30	19	92	0	162	66	175	83
LJ	4	4	1	1	3	1	1	1	3	10	11	5	4	14	21	14	105	136	0	423	396	773
XT	2	4	0	3	8	0	1	0	9	7	2	6	2	5	25	16	45	72	536	0	186	481
LL	13	12	2	4	37	7	5	11	29	27	17	14	21	52	79	27	142	180	308	319	0	1032
LJ	4	6	0	1	2	2	1	1	4	4	2	1	3	16	23	7	46	69	562	501	1032	0

Figure 8: Toll station hourly travel demand.

Table 3: Default parameter settings.

Parameter	Value	Data source
C_1	\$1,000,000	References [30, 44] and South California News https://www.mercurynews.com/
C_2	\$2,000,000	
s	0.5%/km	Most EVs are currently capable of approximately 100-250 miles of driving before recharging (data source: UC Davis; https://phev.ucdavis.edu/)
l	1 km	A selected min. Length of a charging segment on the freeway considering the power transmitter cost (data source: South California News, https://www.mercurynews.com/)
v	60 km/h	The operating speed on the freeway (http://www.0512s.com/lukuang/G94.html)
p^H	100%	—
p^L	20%	Safety suggestions from EV enterprises (e.g., Beijing Automotive Group Co.)

much more in equilibrium than before using this proposed method. After using the proposed method, the charging demand volume is mainly lower than 1200 and evenly distributed on each charging lane. Moreover, the charging volume capacity is more evenly distributed on each charging lane than before using this proposed method. The results indicate that the proposed optimization model can significantly improve the performance of DWCSs and increase the utilization of charging facilities. Figure 11 shows the varying charging demand volume and optimal charging locations for vehicles with different power levels.

Table 4 shows a comparison between the numbers of lanes before and after applying this proposed method. The numbers of DWC lanes in the location range of 50-79, 199-202, and 272-284 decreased, reducing these segments' total construction cost. The original length of these segments would be $(169 * 1 + 44 * 2) \cdot C_1 = 2.7\,\text{km} \cdot \text{lane}$, $(119 * 1 + 44 * 2)\, C_1 = 207\,\text{km} \cdot \text{lane}$, and this process reduces the total amount to a £163 km·lane construction fee, saving approximately \$44,000,000. In this operational deployment process, we reduced the unnecessary charging activities (i.e., vehicles whose battery power level is sufficient for the upcoming trip). This saved resources to provide more space to meet the urgent charging demand. From Table 4, it can be seen that the average current power levels for all vehicles slightly decrease after applying this proposed method. Compared to before using this proposed method, the average current power levels for all vehicles decreased by approximately 0.67% to 25.54% after applying this proposed method. Since DWC is less efficient and economical than plug-in or static charging modes [37, 46], these changes are acceptable because they can increase power utilization efficiency.

To show the operational charging process more clearly, the initial battery levels in this example are normally distributed (i.e., $p_u^0 \sim N(0.65, 0.2)$). Based on the location model results and the proposed methodology, we obtain the approximate optimal solution in the operation process shown in Figure 11, which shows the varying charging demand volume and optimal charging locations for vehicles with different power levels.

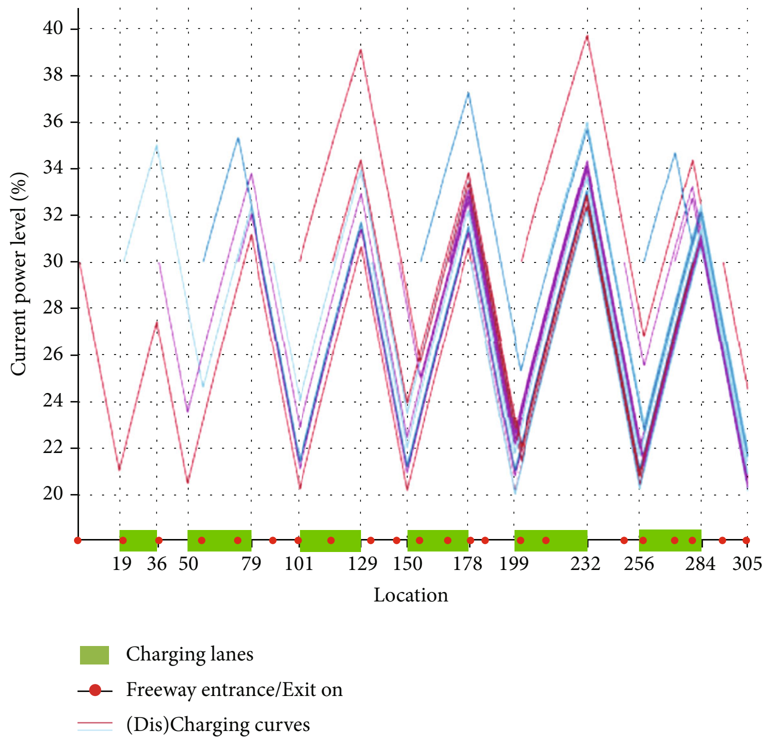

FIGURE 9: Discharging and charging curves for $u \in \mathcal{U}$.

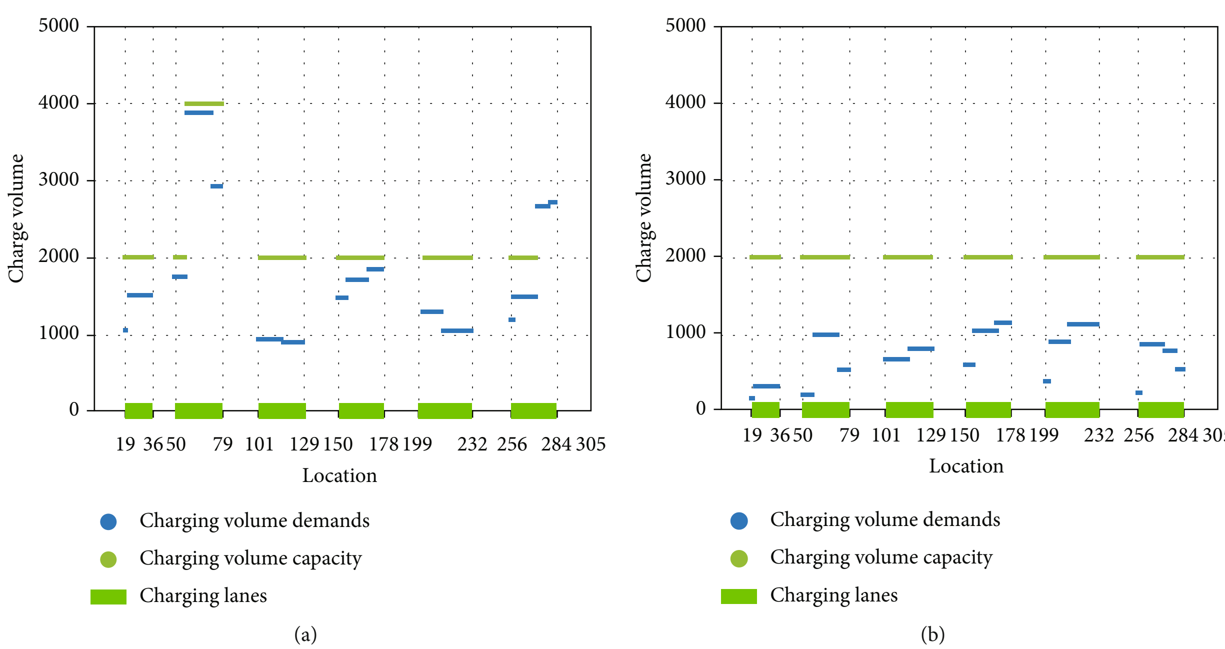

FIGURE 10: DWC lane deployment comparison (a) before and (b) after.

As observed from Figure 11, when the initial power level is in the 30-40% range, the charging demand volume is mostly distributed between 80 and 230, with a relatively even distribution of charging locations from 0 to 300. When the initial power level is in the 40-50% range, the charging demand volume is mostly distributed between 20 and 350, with a relatively even distribution of charging locations from 0 to 300. When the initial power level is in the 50-60% range, the charging demand volume is mostly distributed between 20 and 280, with a relatively even distribution of charging locations from 50 to 290. When the initial power level is in the 60-70% range, the charging demand volume is mostly distributed between 20 and 220,

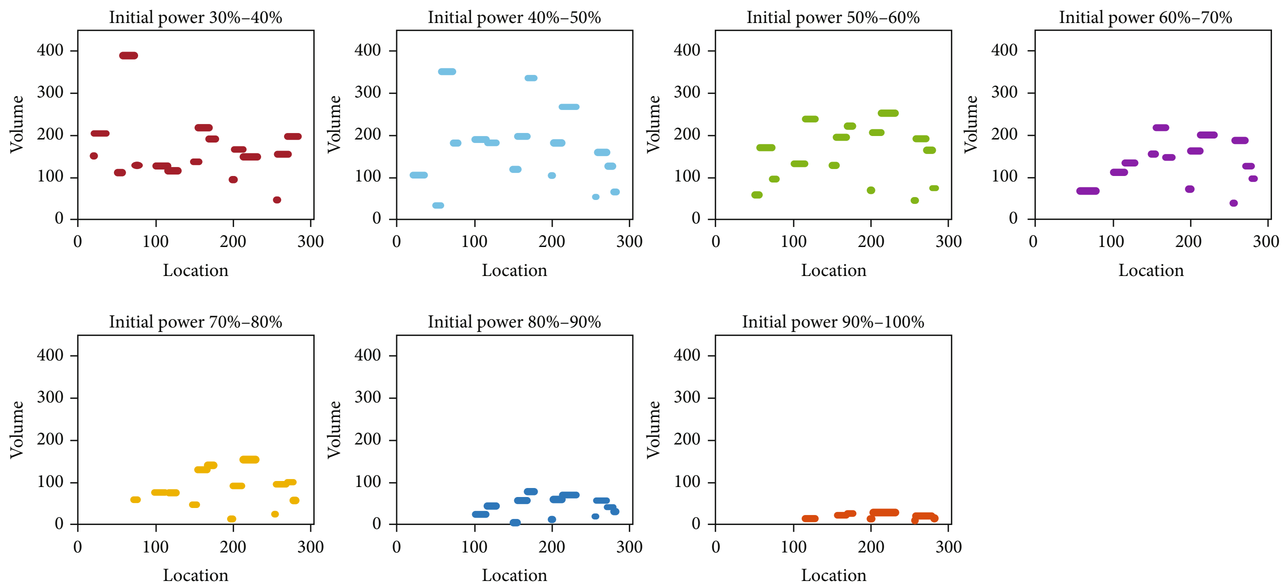

Figure 11: Charging strategies for EVs with varying initial battery levels.

Table 4: Result comparison (number of lanes).

Location range	Number of lanes			Av. current power level	
	Before	After		Before	After
19-21	1	1		51.12%	50.78%
21-36	1	1		58.80%	53.82%
50-57	2	1	↓	54.27%	44.72%
57-73	2	1	↓	59.66%	50.33%
73-79	2	1	↓	61.42%	51.93%
101-116	1	1		53.06%	41.44%
116-129	1	1		57.12%	42.53%
150-156	1	1		52.37%	43.77%
156-169	1	1		56.07%	44.98%
169-178	1	1		58.91%	44.96%
199-202	2	1	↓	50.97%	42.02%
202-214	1	1		53.83%	42.22%
214-232	1	1		57.92%	42.94%
256-258	1	1		50.56%	38.63%
258-272	1	1		55.36%	43.70%
272-280	2	1	↓	59.28%	50.81%
280-284	2	1	↓	60.45%	50.75%

with a relatively even distribution of charging locations from 60 to 290. When the initial power level is in the 70-80% range, the charging demand volume is mostly distributed between 10 and 190, with a relatively even distribution of charging locations from 80 to 290. When the initial power level is in the 80-90% range, the charging demand volume is mostly distributed between 0 and 90, with a relatively even distribution of charging locations from 100 to 290. When the initial power level is in the 90-100% range, the charging demand volume is mostly distributed between 0 and 20, with a relatively even distribution of charging locations from 110 to 290. Therefore, as the initial power level increases, the charging demand volume gradually decreases and the charge position gradually changes to between 100 and 300.

Cost is a very important factor in the optimization of DWCSs for electric vehicles and has been considered in many relevant studies. The results show that reducing the infrastructure cost of DWCSs can attract more electric vehicle users, which is beneficial for reducing carbon emissions and environmental pollution. Moreover, with DWC technology, a vehicle is inductively charged as it moves along a roadway, extending the vehicle range and reducing or eliminating the need for lengthy stops to recharge. The outcome of this study indicates that using our model, a balanced relationship between charging lanes and lane length can be achieved to obtain the optimal number of lanes and lane length. As a result, the efficiency of vehicle charging and the utilization of the DWCS are greatly improved.

The large-scale deployment of internal combustion engine-based vehicles in transport systems leads to the release of harmful fumes into the atmosphere, leading to global warming and climate change, which is the main concern of the global community. The widespread application of DWCS can solve the problem of decreasing the dependence on fossil fuel-based energy sources and reducing their harmful impact on the atmosphere. The DWCS can also effectively solve the problem of difficult charging and the long charging time of electric vehicles, thus promoting the sales and use of electric vehicles. Moreover, the DWCS provides an automatic and effective charging system for future driverless electric vehicles without human intervention.

7. Conclusion

With DWC technology, a vehicle is inductively charged as it moves along a roadway, extending the vehicle range and reducing or eliminating the need for lengthy stops to recharge. Based on DWC technology, a DWCS concept is proposed to overcome the difficulties in setting the charging lanes' location, length, and number and simultaneously consider the varying battery charging rates. To realize the optimal DWCS design, we develop a model to balance the tradeoff between the charging lane location and length and then propose a methodology to reach an approximate optimal number of lanes. This division into two stages can significantly decrease the algorithm complexity and allows the algorithm to quickly obtain an acceptable real-case solution. A numerical example from a Guangdong freeway demonstrates the effectiveness of our model and methodology.

This study can be extended in several directions. Future research can explore the integrated model with dynamic and stochastic demands of EVs, more complicated multitype charging strategies, and their combinations. Additionally, more charging fees and subsidy combinations that consider user equilibrium can be proposed. Moreover, this study would be more applicable when more efficient and customized solution methodologies are introduced to fit the real-time solving speed. Furthermore, it would be interesting to examine the impact of combinations of autonomous, modular, and EV technologies into this DWCS with allowing these vehicles to participate in peak shaving and valley filling to improve unreasonable charging and discharging.

Data Availability

There is no data to support the findings of this study

Conflicts of Interest

The authors declare they have no known competing financial interests or personal relationships that could have appeared to influence the work reported in this paper.

Acknowledgments

This work is supported by the National Natural Science Foundation of China (71971015).

References

[1] Z. Sun and X. Zhou, "To save money or to save time: Intelligent routing design for plug-in hybrid electric vehicle," *Transp. Res. Part D Transp. Environ.*, vol. 43, no. 2011, pp. 238–250, 2016.

[2] International Energy Agency, *Global EV Outlook 2019*, International Energy Agency, 2019.

[3] N. Mouhrim, A. El Hilali Alaoui, and J. Boukachour, "Optimal allocation of wireless power transfer system for electric vehicles in a multipath environment," in *2016 3rd International Conference on Logistics Operations Management (GOL)*, pp. 1–7, Fez, Morocco, 2016.

[4] Z. Chen, F. He, and Y. Yin, "Optimal deployment of charging lanes for electric vehicles in transportation networks," *Transportation Research Part B: Methodological*, vol. 91, pp. 344–365, 2016.

[5] Z. Liu and Z. Song, "Robust planning of dynamic wireless charging infrastructure for battery electric buses," *Transportation Research Part C: Emerging Technologies*, vol. 83, pp. 77–103, 2017.

[6] M. Zhao, X. Li, J. Yin, J. Cui, L. Yang, and S. An, "An integrated framework for electric vehicle rebalancing and staff relocation in one-way carsharing systems: model formulation and Lagrangian relaxation- based solution approach," *Transportation Research Part B: Methodological*, vol. 117, pp. 542–572, 2018.

[7] W. Sierzchula, S. Bakker, K. Maat, and B. Van Wee, "The influence of financial incentives and other socio-economic factors on electric vehicle adoption," *Energy Policy*, vol. 68, pp. 183–194, 2014.

[8] A. Chen, Z. Zhou, P. Chootinan, S. Ryu, C. Yang, and S. C. Wong, "Transport network design problem under uncertainty: a review and new developments," *Transport Reviews*, vol. 31, no. 6, pp. 743–768, 2011.

[9] Y. Nie and M. Ghamami, "A corridor-centric approach to planning electric vehicle charging infrastructure," *Transportation Research Part B: Methodological*, vol. 57, pp. 172–190, 2013.

[10] F. Deflorio, P. Guglielmi, I. Pinna, L. Castello, and S. Marfull, "Modeling and analysis of wireless "charge while driving" operations for fully electric vehicles," *Transportation Research Procedia*, vol. 5, pp. 161–174, 2015.

[11] N. Mohamed, F. Aymen, T. E. A. Alharbi et al., "A comprehensive analysis of wireless charging systems for electric vehicles," *IEEE Access*, vol. 10, pp. 43865–43881, 2022.

[12] N. Mohamed, F. Aymen, M. Alqarni et al., "A new wireless charging system for electric vehicles using two receiver coils," *Ain Shams Engineering Journal*, vol. 13, no. 2, article 101569, 2022.

[13] N. Mohamed, F. Aymen, A. Altamimi, Z. A. Khan, and S. Lassaad, "Power management and control of a hybrid electric vehicle based on photovoltaic, fuel cells, and battery energy sources," *Sustain*, vol. 14, no. 5, 2022.

[14] Y. J. Jang, "Survey of the operation and system study on wireless charging electric vehicle systems," *Transportation Research Part C: Emerging Technologies*, vol. 95, pp. 844–866, 2018.

[15] N. Mohamed, F. Aymen, and M. Alqarni, "Inductive power transmission system for electric car charging phase: modeling plus frequency analysis," *World Electric Vehicle Journal*, vol. 12, no. 4, 2021.

[16] V. Etacheri, R. Marom, R. Elazari, G. Salitra, and D. Aurbach, "Challenges in the development of advanced Li-ion batteries: a review," *Energy & Environmental Science*, vol. 4, no. 9, pp. 3243–3262, 2011.

[17] A. Reatti, F. Corti, L. Pugi et al., "Application of induction power recharge to garbage collection service," in *2017 IEEE 3rd International Forum on Research and Technologies for Society and Industry (RTSI)*, pp. 1–5, Modena, Italy, 2017.

[18] T. M. Fisher, K. B. Farley, Y. Gao, H. Bai, and Z. T. H. Tse, "Electric vehicle wireless charging technology: a state-of-the-art review of magnetic coupling systems," *Wireless Power Transfer*, vol. 1, no. 2, pp. 87–96, 2014.

[19] C. C. Mi, G. Buja, L. Fellow, S. Y. Choi, C. T. Rim, and S. Member, "Modern advances in wireless power transfer systems for roadway powered electric vehicles," *IEEE*

Transactions on Industrial Electronics, vol. 63, no. 10, pp. 6533–6545, 2016.

[20] D. De Marco, A. Dolara, and M. Longo, "Design and performance analysis of pads for dynamic wireless charging of EVs using the finite element method," *Energies*, vol. 12, no. 21, p. 4139, 2019.

[21] L. Mihet-popa and S. Member, "Inductive wireless power transfer charging for electric vehicles–a review," *IEEE Access*, vol. 9, pp. 137667–137713, 2021.

[22] F. Corti, A. Reatti, A. Nepote et al., "A secondary-side controlled electric vehicle wireless charger," *Energies*, vol. 13, no. 24, 2020.

[23] K. N. Mude and K. Aditya, "Comprehensive review and analysis of two-element resonant compensation topologies for wireless inductive power transfer systems," *Chinese Journal of Electrical Engineering*, vol. 5, no. 2, pp. 14–31, 2019.

[24] S. Sun, Z. Liu, Y. Hou et al., "Analysis of harmonic characteristics based on improved double-LCC compensation network structure," *Energy Reports*, vol. 8, pp. 891–902, 2022.

[25] L. Pugi, A. Reatti, and F. Corti, "Application of wireless power transfer to railway parking functionality: preliminary design considerations with series-series and LCC topologies," *Journal of Advanced Transportation*, vol. 2018, Article ID 8103140, 14 pages, 2018.

[26] F. Corti, L. Paolucci, A. Reatti et al., "A comprehensive comparison of resonant topologies for magnetic wireless power transfer," in *2020 IEEE 20th Mediterranean Electrotechnical Conference (MELECON)*, pp. 582–587, Palermo, Italy, 2020.

[27] J. Hilton, *Qualcomm Demonstrates Dynamic Electric Vehicle Charging*, Automotive Industries AI, 2017.

[28] S Report/Dubai, *Dubai Tests road that Charges your Car as you Drive*, Khaleej Times, 2020.

[29] J. G. Bolger, F. A. Kirsten, and L. S. Ng, "Inductive power coupling for an electric highway system," in *28th IEEE Vehicular Technology Conference*, pp. 137–144, Denver, CO, USA, 1978.

[30] M. Fuller, "Wireless charging in California: range, recharge, and vehicle electrification," *Transportation Research Part C: Emerging Technologies*, vol. 67, pp. 343–356, 2016.

[31] P. Bansal, "Charging of electric vehicles: technology and policy implications," *Journal of Science Policy & Governance*, vol. 6, no. 1, pp. 1–20, 2015.

[32] D. Herron, *Siemens eHighway of the Future Concept*, New Atalas, 2020.

[33] S. Pettersson, J. Andersson, T. Fransson, M. Klingegård, and J. Wedlin, "Large scale testing of wireless charging in Sweden," in *29th World Electric Vehicle Symposium and Exhibition (EVS 2016)*, pp. 1–12, Montreal, Canada, 2016.

[34] J. He, H. Yang, T. Q. Tang, and H. J. Huang, "Optimal deployment of wireless charging lanes considering their adverse effect on road capacity," *Transportation Research Part C: Emerging Technologies*, vol. 111, no. June, p. 171, 2020.

[35] F. He, D. Wu, Y. Yin, and Y. Guan, "Optimal deployment of public charging stations for plug-in hybrid electric vehicles," *Transportation Research Part B: Methodological*, vol. 47, pp. 87–101, 2013.

[36] Y. Alwesabi, Y. Wang, R. Avalos, and Z. Liu, "Electric bus scheduling under single depot dynamic wireless charging infrastructure planning," *Energy*, vol. 213, article 118855, 2020.

[37] S. Jeong, Y. J. Jang, and D. Kum, "Economic analysis of the dynamic charging electric vehicle," *IEEE Transactions on Power Electronics*, vol. 30, no. 11, pp. 6368–6377, 2015.

[38] P. Machura and Q. Li, "A critical review on wireless charging for electric vehicles," *Renewable and Sustainable Energy Reviews*, vol. 104, pp. 209–234, 2019.

[39] R. Riemann, D. Z. W. Wang, and F. Busch, "Optimal location of wireless charging facilities for electric vehicles: flow capturing location model with stochastic user equilibrium," *Transportation Research Part C: Emerging Technologies*, vol. 58, Part A, pp. 1–12, 2015.

[40] I. Hwang, Y. J. Jang, Y. D. Ko, and M. S. Lee, "System optimization for dynamic wireless charging electric vehicles operating in a multiple-route environment," *IEEE Transactions on Intelligent Transportation Systems*, vol. 19, no. 6, pp. 1709–1726, 2018.

[41] B. Sun and D. H. K. Tsang, "Performance analysis of dynamic wireless charging system for electric vehicles: a queueing approach," in *e-Energy '17: Proceedings of the Eighth International Conference on Future Energy Systems*, pp. 168–178, 2017.

[42] Y. D. Ko and Y. J. Jang, "The optimal system design of the online electric vehicle utilizing wireless power transmission technology," *IEEE Transactions on Intelligent Transportation Systems*, vol. 14, no. 3, pp. 1255–1265, 2013.

[43] Y. J. Jang, S. Jeong, and Y. D. Ko, "System optimization of the on-line electric vehicle operating in a closed environment," *Computers and Industrial Engineering*, vol. 80, pp. 222–235, 2015.

[44] Y. D. Ko, Y. J. Jang, and M. S. Lee, "The optimal economic design of the wireless powered intelligent transportation system using genetic algorithm considering nonlinear cost function," *Computers and Industrial Engineering*, vol. 89, pp. 67–79, 2015.

[45] Y. J. Jang, E. S. Suh, and J. W. Kim, "System architecture and mathematical models of electric transit bus system utilizing wireless power transfer technology," *IEEE Systems Journal*, vol. 10, no. 2, pp. 495–506, 2016.

[46] Y. J. Jang, S. Jeong, and M. S. Lee, "Initial energy logistics cost analysis for stationary, quasi-dynamic, & dynamicwireless charging public transportation systems," *Energies*, vol. 9, no. 7, 2016.

[47] Z. Chen, W. Liu, and Y. Yin, "Deployment of stationary and dynamic charging infrastructure for electric vehicles along traffic corridors," *Transportation Research Part C: Emerging Technologies*, vol. 77, pp. 185–206, 2017.

[48] P. W. Chen and Y. M. Nie, "Analysis of an idealized system of demand adaptive paired-line hybrid transit," *Transportation Research Part B: Methodological*, vol. 102, pp. 38–54, 2017.

[49] M. S. Lee and Y. J. Jang, "Charging infrastructure allocation for wireless charging transportation system," in *Proceedings of the Eleventh International Conference on Management Science and Engineering Management*, pp. 1630–1644, 2018.

[50] Z. Pantic, S. Bai, and S. M. Lukic, "Inductively coupled power transfer for continuously powered electric vehicles," in *2009 IEEE Vehicle Power and Propulsion Conference*, pp. 1271–1278, Dearborn, MI, USA, 2009.

[51] S. Y. Choi, B. W. Gu, S. Y. Jeong, and C. T. Rim, "Advances in wireless power transfer systems for roadway-powered electric vehicles," *IEEE Journal of Emerging and Selected Topics in Power Electronics*, vol. 3, no. 1, pp. 18–36, 2015.

[52] C. Mi, M. A. Masrur, and D. W. Gao, *Hybrid Electric Vehicles: Principles and Applications with Practical Perspectives*, John Wiley & Sons, 2011.

[53] S. Mohrehkesh and T. Nadeem, "Toward a wireless charging for battery electric vehicles at traffic intersections," in *2011 14th International IEEE Conference on Intelligent Transportation Systems (ITSC)*, pp. 113–118, Washington, DC, USA, 2011.

[54] W. Zhang, H. Zhao, and M. Xu, "Optimal operating strategy of short turning lines for the battery electric bus system," *Communications in Transportation Research*, vol. 1, article 100023, 2021.

[55] L. Yue, M. Abdel-Aty, and Z. Wang, "Effects of connected and autonomous vehicle merging behavior on mainline human-driven vehicle," *Journal of Intelligent and Connected Vehicles*, vol. 5, no. 1, pp. 36–45, 2022.

[56] X. G. Yang, G. Zhang, S. Ge, and C. Y. Wang, "Fast charging of lithium-ion batteries at all temperatures," *Proceedings of the National Academy of Sciences of the United States of America*, vol. 115, no. 28, pp. 7266–7271, 2018.

[57] D. Ouyang, M. Chen, J. Liu, R. Wei, J. Weng, and J. Wang, "Investigation of a commercial lithium-ion battery under overcharge/over-discharge failure conditions," *RSC Advances*, vol. 8, no. 58, pp. 33414–33424, 2018.

[58] Z. Chen, B. Xia, C. C. Mi, and R. Xiong, "Loss-minimization-based charging strategy for lithium-ion battery," *IEEE Transactions on Industry Applications*, vol. 51, no. 5, pp. 4121–4129, 2015.

[59] X. Wu, D. Freese, A. Cabrera, and W. A. Kitch, "Electric vehicles' energy consumption measurement and estimation," *Transportation Research Part D: Transport and Environment*, vol. 34, pp. 52–67, 2015.

[60] H. Zhang, C. J. R. Sheppard, T. E. Lipman, and S. J. Moura, "Joint fleet sizing and charging system planning for autonomous electric vehicles," *IEEE Transactions on Intelligent Transportation Systems*, vol. 21, no. 11, pp. 4725–4738, 2020.

[61] J. J. Cochran, L. A. Cox Jr., P. Keskinocak, J. P. Kharoufeh, and J. C. Smith, "MILP software," in *Wiley Encyclopedia of Operations Research and Management Science*, John Wiley & Sons, Inc., 2011.

[62] Y. Zhang, A. D'Ariano, B. He, and Q. Peng, "Microscopic optimization model and algorithm for integrating train timetabling and track maintenance task scheduling," *Transportation Research Part B: Methodological*, vol. 127, pp. 237–278, 2019.

[63] M. Fuentes, L. Cadarso, and Á. Marín, "A hybrid model for crew scheduling in rail rapid transit networks," *Transportation Research Part B: Methodological*, vol. 125, pp. 248–265, 2019.